CHAPTER II
LITERATURE REVIEW

2.1 Background

So far, the increasing of energy requirement together with lacking of fossil fuels motivates many researchers to focus on the new energy source as the alternative source for avoiding the global warming crisis. Hydrogen is described as a primary alternative energy including many advantages. For example, it can be produced from renewable sources such as biomass, solar energy and so on. Practically, PEM fuel cells are the main unit for converting hydrogen to electricity with high efficiency (Faungnawakij et al., 2006). Compared with the fossil fuel, hydrogen was defined as a clean energy within environmentally friendly in term of non-emission of greenhouse gases. To keep searching for techniques in providing the high purity of hydrogen in PEM fuel cells usage, the hydrogen production must be evaluated for both optimum process and condition.

2.2 Hydrogen Production

Hydrogen, the most abundant element normally forming as a compound with other elements, is widely applied in PEM fuel cells by reacting with oxygen to create H_2O. Along hydrogen production process, molecule of water and other raw materials are splitting in to H_2, CO, and CO_2 by compressing hydrogen in reforming process. Among the raw materials, methanol is regarded as one of the most promising candidates for the on-board reforming to the high purity hydrogen.

Methanol (CH_3OH) is recommended to be the feed stock to produce hydrogen and has received great attention due to an anticipated hydrogen energy. Methanol can be obtained by many varieties of feed stocks such as coal, natural gas, and syn-gas. Moreover, methanol can also be converted from agricultural wastes (biomass) as an alternative way to manage agricultural waste. Interestingly, the reasons why methanol to be considered as the best storable form of hydrogen are the conversion taking place at relatively low temperatures, high hydrogen-to-carbon

ratio, the absence of C–C bond (thus minimizing coke formation), and no sulfur contaminating in the product streams. Conventionally, methanol reforming plays as important role for converting methanol to hydrogen. This process can be classified into 3 main techniques; steam reforming of methanol (SRM), partial oxidation of methanol (POM), and oxidative steam reforming of methanol (combination of SRM and POM, ORSM). Nevertheless, our experiments mainly focused on the hydrogen production in the OSRM reaction as a function of temperature (200–400°C).

2.2.1 Methanol Steam Reforming (SRM)

Steam reforming is an endothermic reaction, which is favorable at high temperature (250–350°C), and low pressure (Armor. 1999). Thus, the reaction requires energy input, which makes transient operation difficult when bursts of energy are needed. This reaction reacts between hydrocarbon fuel and water and also is the most extensively studied process due to its highest hydrogen yield and high composition toward carbon dioxide. The overall reaction for SRM is shown in Eq. 2.1.

$$CH_3OH(g) + H_2O(g) \rightarrow 3H_2(g) + CO_2(g) \quad \Delta H°_R = +49.5 \text{ kJmol}^{-1} (25°C) \quad (2.1)$$
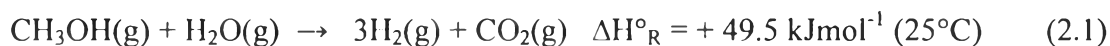
When using stoichiometric feedstock, the SRM ideally produces only H_2 and CO_2. However, to perform complete SRM, decomposition of methanol (DCM) and water gas shift (WGS) will be combined to form complete SRM reaction (Eq. 2.2-2.3)

$$CH_3OH(g) \rightarrow 2H_2(g) + CO(g) \quad DCM \quad \Delta H°_R = +91.6 \text{ kJmol}^{-1} (25°C) \quad (2.2)$$

$$CO(g) + H_2O(g) \rightarrow H_2(g) + CO_2(g) \quad WGSR \quad \Delta H°_R = -41.1 \text{ kJmol}^{-1} (25°C) \quad (2.3)$$

Perez et al. (2007) suggests that Cu-based catalysts provide high CO selectivity and undesirable CO in the SRM. This is attributed to a reaction pathway, where adsorbed intermediate HCHO (formaldehyde) species react with water to

directly produce H_2 and CO_2 without forming a CO intermediate. In addition, CO and CH_4 could be sources of coke formation or a carbonaceous deposition (Manzoli *et al.*, 2004) over the steam reforming catalysts, leading to the deactivation of catalysts. And CH_4 can also be formed from by-product of SRM reaction.

$$(CH_3)_2O + 2H_2 \rightarrow 2CH_4 + H_2O \tag{2.4}$$

There are two major pathways for coke (carbon) formation (Armor. 1999):

$$2CO \rightarrow CO_2 + C \tag{2.5}$$

$$CH_4 \rightarrow C + 2H_2 \tag{2.6}$$

To avoid risk of coke formation researchers keep going on development of catalyst which exhibit more efficiency CO oxidation to minimize CO formation.

2.2.1.1 Experimental Condition

Effect of reaction temperature is shown in Figure 2.1. Along the increment of reaction temperature, the methanol conversion, hydrogen yield, and carbon monoxide gradually increased and methanol was almost converted at 280°C.
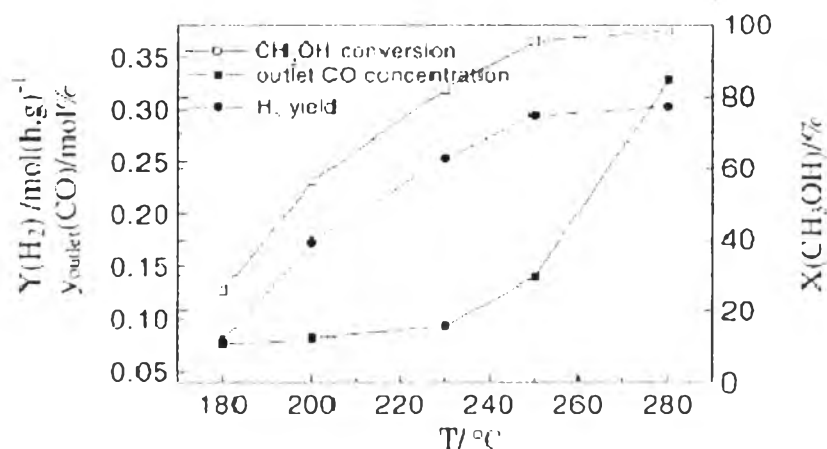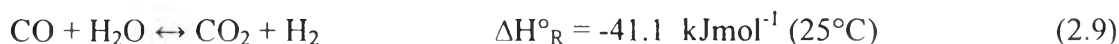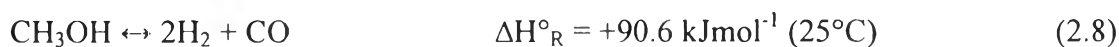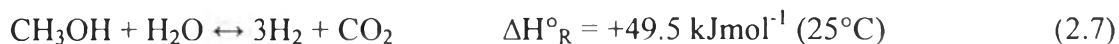

Figure 2.1 Effect of reaction temperature in methanol steam reforming reaction (Zhang and Shi. 2003).

2.2.1.2 Mechanism of Methanol Steam Reforming

The kinetic studies and reaction mechanisms data of the SRM process are little available in the literature. The individual reactions as shown in below equations related to the kinetic model are still under debated.

$$CH_3OH + H_2O \leftrightarrow 3H_2 + CO_2 \qquad \Delta H^\circ_R = +49.5 \text{ kJmol}^{-1} (25^\circ C) \qquad (2.7)$$

$$CH_3OH \leftrightarrow 2H_2 + CO \qquad \Delta H^\circ_R = +90.6 \text{ kJmol}^{-1} (25^\circ C) \qquad (2.8)$$

$$CO + H_2O \leftrightarrow CO_2 + H_2 \qquad \Delta H^\circ_R = -41.1 \text{ kJmol}^{-1} (25^\circ C) \qquad (2.9)$$
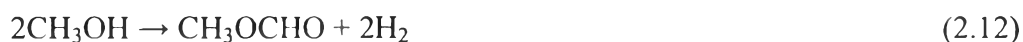
To form SRM reaction DCM and WGSR were combined. However, CO is a by-product from SRM reaction that was almost produced from DCM reaction (Eq. 2.10).

$$CH_3OH(g) \rightarrow 2H_2(g) + CO(g) \qquad \Delta H^\circ_R = +91.6 \text{ kJmol}^{-1} \qquad (2.10)$$

WGSR is usually operated with excess steam in the reformer in order to lower the CO concentration in the product gas. Nevertheless, the formation of undesired by-product gases in reforming process are depend on operating conditions and type of catalyst. The formation of methane consumes hydrogen from methanol and steam, suppressing the production of hydrogen gas (Eq. 2.11).

$$CO(g) + H_2O(g) \rightarrow H_2(g) + CO_2(g) \qquad \Delta H^\circ_R = -41 \text{ kJmol}^{-1} \qquad (2.11)$$

Jiang et al. (1993) proposed the elementary surface reaction mechanisms and derived the Langmuir–Hinshelwood expression. They suggested that CO_2 was formed via decomposition of methyl formate (Eq. 2.12–2.14).

$$2CH_3OH \rightarrow CH_3OCHO + 2H_2 \qquad (2.12)$$

$$CH_3OCHO + H_2O \rightarrow HCOOH + CH_3OH \qquad (2.13)$$

$$HCOOH \rightarrow CO_2 + H_2 \qquad (2.14)$$

Interestingly, they neglected the CO formation that cannot be neglected even if very low concentration because it can poison the Pt anode of PEM fuel cell.

Breen *and Ross*. (1999) studied CO formation mechanism through DRIFT analysis and confirmed that the CO formation over $CuO/ZnO/ZrO_2/Al_2O_3$ catalyst for steam reforming of methanol occurs via reverse water gas shift reaction (Eq. 2.15). Recently, many researchers have also proposed the CO formation via reverse water gas shift reaction (RWGS) that uses the products of the reforming reaction i.e. H_2 and CO_2.

$$CO_2 + H_2 \leftrightarrow CO + H_2O \qquad \Delta H^{\circ}_R = +41.1 \text{ kJmol}^{-1} (25^{\circ}C) \qquad (2.15)$$

Trimm *et al.* (1994) reported that CeO_2 is such a strong reducing reagent that it can decompose water into hydrogen; therefore, water can be activated by the reduced ceria. It is noted that the production of CO_2 consumes one site surface of oxygen. Men *et al.* (2004) depicted schematically in Figure 2.2 involves with four distinct steps: (i) the adsorption of methanol and water at the Cu/CeO_2 interface, (ii) the surface reaction and the desorption of gaseous products, (iii) the migration of surface oxygen from CeO_2 to the reduced Cu (oxygen reverse spillover), (iv) the regeneration of partially oxidized copper and oxygen vacancies.
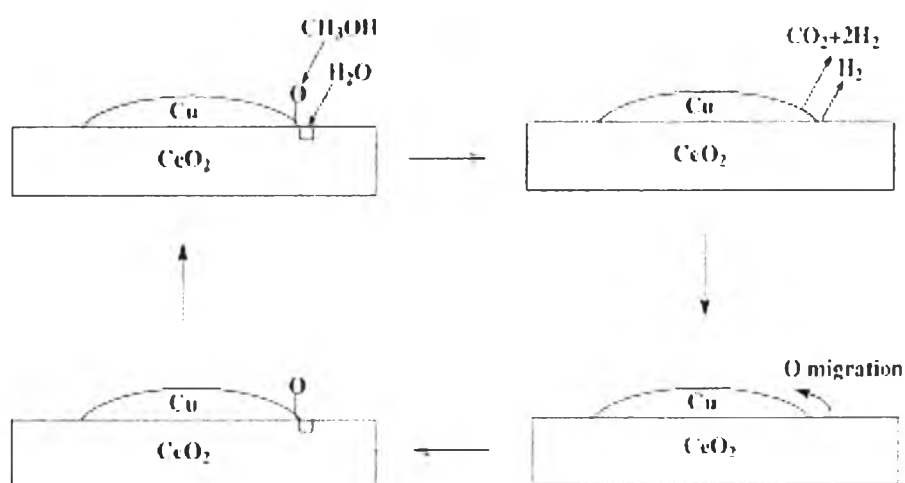

Figure 2.2 Proposed reaction mechanism for SRM at the Cu/CeO_2 interface (Men *et al.*, 2004).

2.2.2 Partial Oxidation of Methanol (POM)

Partial oxidation of methanol is another possibility to produce H_2 which has a higher reaction rate than steam reforming. Moreover, it can produce half the hydrogen selectivity. Furthermore, POM is highly exothermic; therefore, temperature control can be difficult. Partial oxidation reaction is a reaction that fuel was partially oxidized to CO and H_2. There are several advantages of this mechanism over steam reforming. For instance, there is no steam required and have higher rate of reaction compared to steam reforming process. (Pinzari et al., 2006). The reaction of POM is shown in Eq. 2.16

$$CH_3OH(g) + 1/2O_2(g) \rightarrow 2H_2(g) + CO_2(g) \quad \Delta H^\circ_R = -192 \text{ kJmol}^{-1} (25^\circ C) \quad (2.16)$$
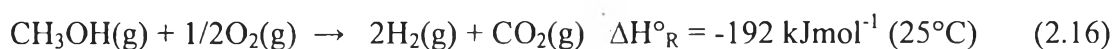
Copper-zinc catalysts have been found to be very active for the partial oxidation of methanol. The onset of the partial oxidation reaction is 215°C and the rates of methanol and oxygen conversion increase strongly with increasing temperature to selectivity produce H_2 and CO_2 (Figure 2.3). The rate of CO formation was very low throughout the temperature range explored (200–225°C) and H_2O formation decreased for temperature above 215°C. As a general rule, methanol conversion to H_2 and CO_2 increased with copper content, reaching a maximum with $Cu_{40}Zn_{60}$ catalyst and decreasing for higher copper loadings. The $Cu_{40}Zn_{60}$ catalyst with the highest copper metal area was the most active and selective for the partial oxidation of methanol. On the contrary, non-reduced catalysts prior to the reaction displayed very low activity, CO_2 and H_2O were the main products while only a few of H_2 was presented. The activity data in the POM to H_2 and CO_2 over Cu/ZnO catalysts obtained with different catalyst compositions and different Cu^0 metal surface areas revealed that the reaction depend on the presence of both phases, ZnO and Cu^0. On the other hand, for the catalysts with Cu concentrations in the range of 40–60 wt%, the copper metal surface area seems to be the main factor determining the reaction rate (Fierro et al., 1998).
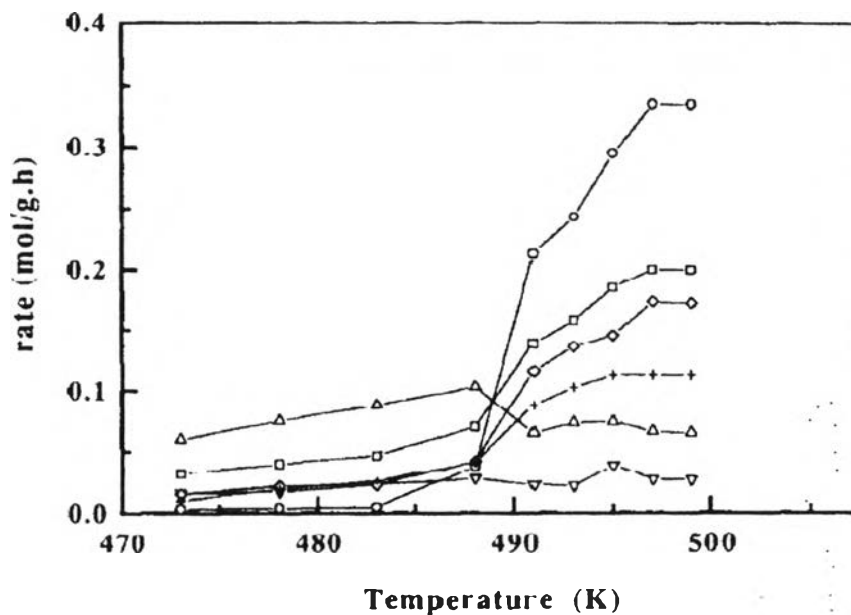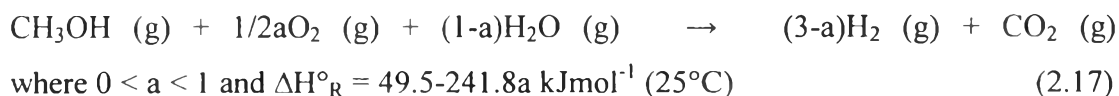
Figure 2.3 Partial oxidation of methanol over the $Cu_{40}Zn_{60}$: ($\square$), CH_3OH conversion; (+), O_2 conversion; ($\circ$), H_2; ($\Diamond$), CO_2; ($\triangle$), H_2O;(v), CO (Alejo L. *et al.*, 1997).

2.2.3 Oxidative Steam Reforming of Methanol (OSRM)

Oxidative steam reforming is the combination of steam reforming (SRM) and partial oxidation (POM). Difference in heat of reaction reflects the heat exchanging between endothermic reaction (steam reforming) and exothermic reaction (partial oxidation), which creates sufficient heat to stabilize each other and improve efficiency of H_2 production. The reaction of oxidative steam reforming of methanol is shown in Eq. 2.17.

$$CH_3OH \ (g) \ + \ 1/2aO_2 \ (g) \ + \ (1\text{-}a)H_2O \ (g) \quad \rightarrow \quad (3\text{-}a)H_2 \ (g) \ + \ CO_2 \ (g)$$

where $0 < a < 1$ and $\Delta H^{\circ}_R = 49.5\text{-}241.8a \ kJmol^{-1}$ (25°C) \hfill (2.17)

where a is the stoichiometric coefficient for steam reforming and partial oxidation. In this process, methanol is reacted with a mixture of O_2 and steam in a "thermo reactor" over a catalyst surface.

OSRM process can use the energy produced from POM to supply SRM that the reason why OSRM can be run adiabatically. This eliminates the need to transfer heat across a heat-conducting boundary. In term of reaction rate oxidative steam reforming, by combined steam reforming and partial oxidation, has much more reaction rate than steam reforming and oxygen concentration in the gas phase is the main parameter determining the reactor performance. Perez *et al.*, 2007 suggested an oxidation decomposition followed by reforming scheme for the process. Additionally, they studied OSRM of Cu/CeO_2 with GHSV = 30,000 h^{-1} and found that $2Cu/CeO_2$ was proved to be a good catalyst to produce hydrogen rich gas mixture in the temperature range of 210 to 230°C with high activity in OSRM reaction and the $6Cu/CeO_2$ catalyst had the best performance towards H_2 at higher temperature, as shown in Figure 2.4.
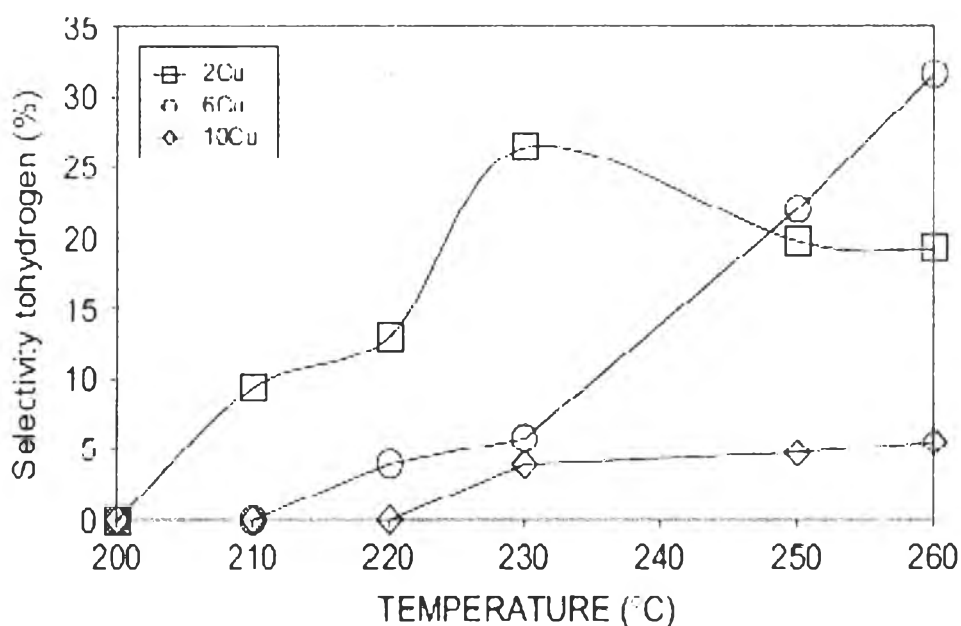

Figure 2.4 Hydrogen selectivity of OSRM over Cu/CeO_2 catalysts with various metal loadings (Perez *et al.*, 2007).

In term of methanol conversion, as illustrated in Figure 2.5, the breakthrough temperature for all catalysts was approximately at 200°C. The activity tended to increase all along increment of temperature until 220°C, after this

temperature all catalyst was less active than 200–220°C. However, the 10Cu/CeO$_2$ catalyst was the less active at every temperature of reaction. The catalytic activity of the samples at 260°C showed the following order: 2Cu/CeO$_2$ ≈ 6Cu/CeO$_2$ > 10Cu/CeO$_2$. Methanol conversion reached almost 100% in the 2Cu and 6Cu catalysts, while in the 10Cu sample only 84% conversion was observed at the maximum reaction temperature.
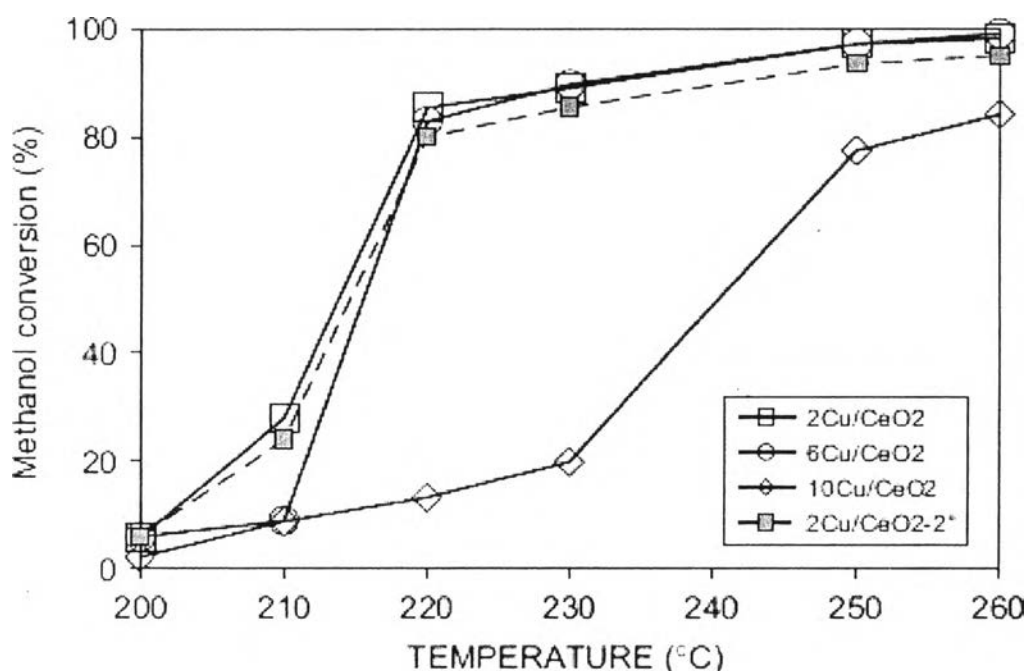

Figure 2.5 Methanol conversion of OSRM over Cu/CeO$_2$ catalysts with various metal loadings (Perez *et al.*, 2007).

Agrell *et al.* (2003) reported that in OSRM reaction at low CO content selectivity of H$_2$ is following toward: SRM > OSRM > POM. However, some alternative catalysts must be designed for producing hydrogen with high yield, generating by the same time with minimizing amounts of CO.

Pinzari *et al.* (2006) performed the effect of gas effluent composition temperature in SRM and OSRM in Figure 2.6 a and b, respectively. Result showed that activity are not occur at 300°C, and above this temperature reactions are strongly influenced by the temperature and complete at 400°C for both methanol and

hydrogen composition. The presence of O_2 in OSRM process does not seem likely to modify the methanol conversion to H_2 and CO_2. In both processes, CO and $(CH_3)_2O$ are formed as by-products while CH_4 is produced in the SRM process.
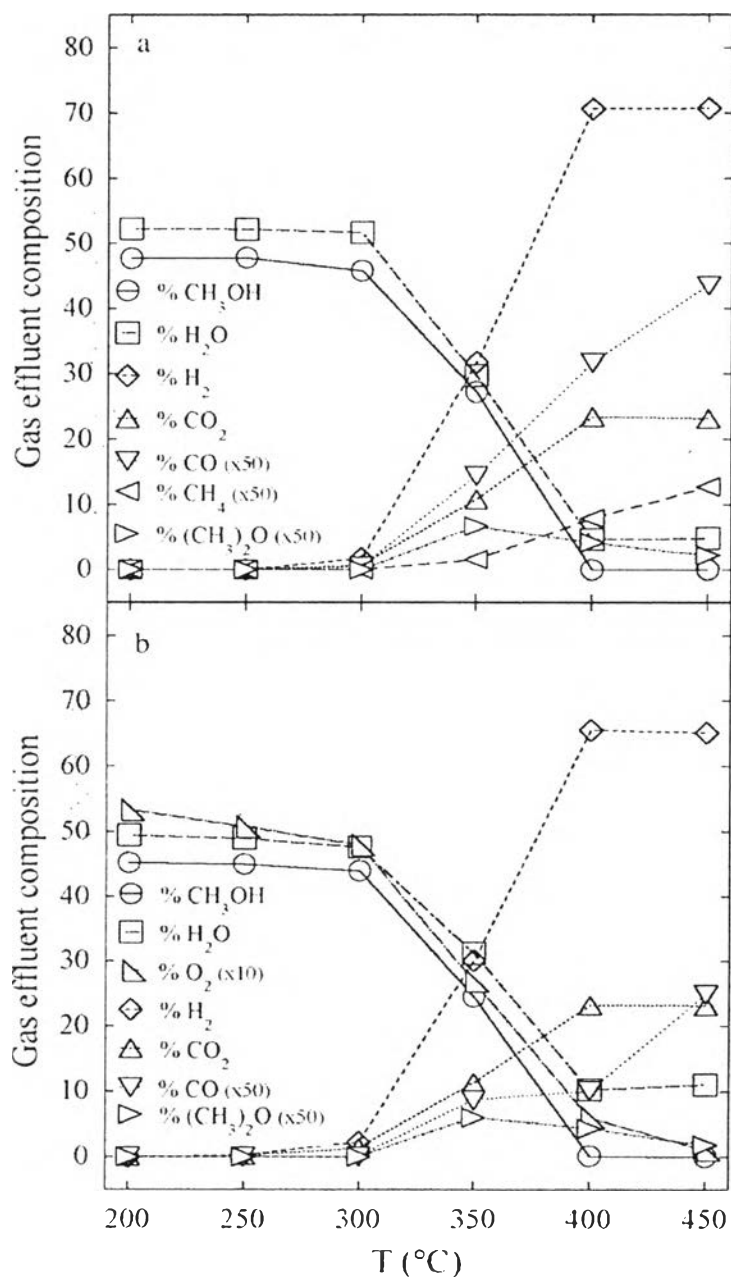

Figure 2.6 Effect of temperature on the gas effluent composition in the SRM (a) and CRM (b) reactions over $Zn_{10}Ti_{90}$ (Pinzari et al.. 2006).

At temperature higher than 350°C, DME can react with H_2 over titania surfaces leading to the formation of methane and water, as shown in Eq. 2.18.

$$(CH_3)_2O + 2H_2 \rightarrow 2CH_4 + H_2O \tag{2.18}$$

This could explain why at temperature higher than 350 °C, DME and CH_4 start increase concurrently in the SRM process. On the contrary, no CH_4 is detected under OSRM reaction because the presence of O_2 suppresses CH_4 formation, as shown in Eq. 2.19.

$$CH_4 + O_2 \rightarrow CO_2 + 2H_2 \tag{2.19}$$

The results also showed that in the OSRM process the CO content is lower than in the SRM process, probably because of its oxidation to CO_2, as shown in Eq. 2.20.

$$CO + 1/2O_2 \rightarrow CO_2 \tag{2.20}$$

Even though adding O_2 doesn't extremely increase the methanol conversion but, it also decrease CO and CH_4 formation, and allowing a higher CO_2 selectivity. At 400°C, when the reactions are complete, selectivity to CO_2 is 96% in the SRM reaction and 96% in the CRM reaction. For a better understanding of the effect of temperature, the methanol conversion and the hydrogen yield, defined as the methanol conversion multiply with H_2 selectivity, are reported in Figure 2.7a and b, respectively, the comparison of the SRM and OSRM data. In Figure 2.7a, the SRM and OSRM reaction initiates to react at 300°C and also have a bit higher methanol conversion than SRM up till 350°C. In Figure 2.7b, hydrogen yields are quite similar in the two different reactions up to 350°C; this is probably due to the compensation between the higher conversion of methanol in case of OSRM reaction and the higher theoretical hydrogen yield in case of the SRM reaction. When the reactions are complete, hydrogen yields are 2.86 and 2.78, in the SRM and CRM reactions, respectively.
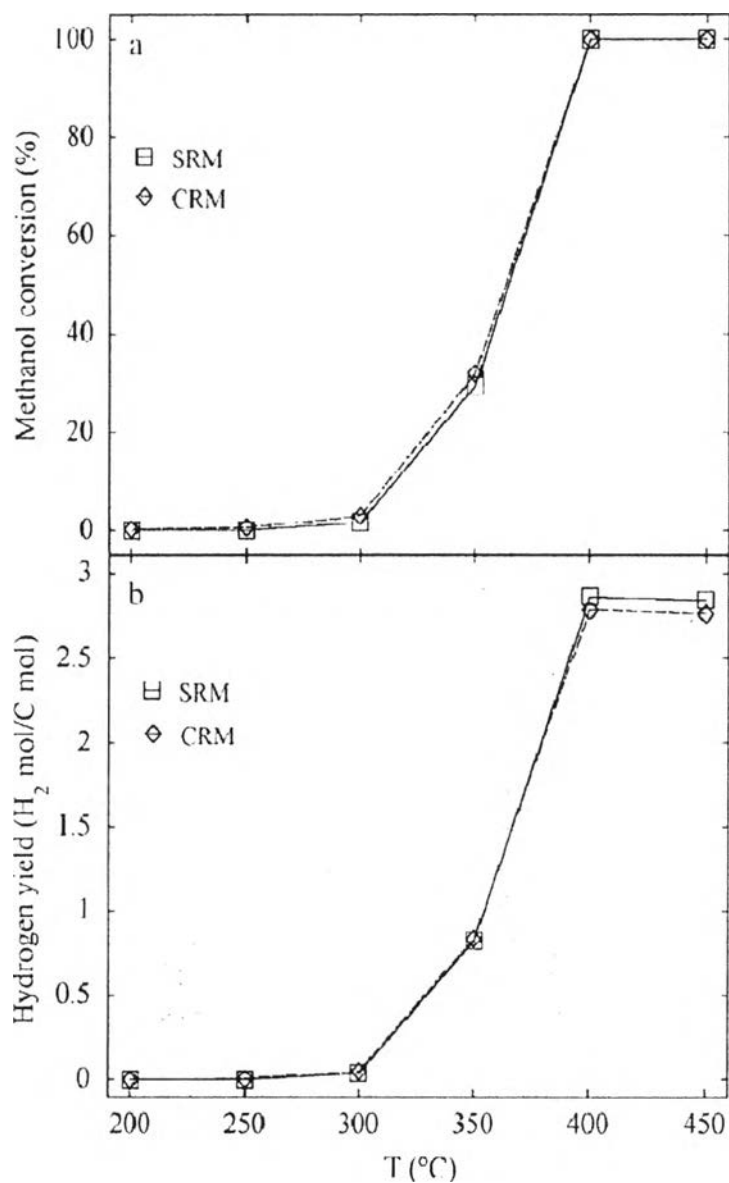
Figure 2.7 Methanol conversion (a) and hydrogen yield (b) as a function of the temperature for $Zn_{10}Ti_{90}$ (Pinzari *et al.*, 2006).

2.3 Gold Catalyst

Gold has long been regarded as a poorly active catalyst. Recently, Gold catalysts have been attracting rapidly due to their potential applicabilities to many reactions of both industrial and environmental importance. It has atomic number 79 and atomic weight 196.967.

Cameron *et al.* (2003) reported that gold catalysts have been used in commercial applications for catalyze reaction, such as:

- oxidation of CO and hydrocarbons,
- water gas shift (WGS),
- reduction of NO with propene, CO, or H_2,
- reactions with halogenated compounds,
- water or H_2O_2 production from H_2 and O_2,
- removal of CO from hydrogen streams,
- hydrochlorination of ethyne,
- selective oxidation, e.g. epoxidation of olefins,
- selective hydrogenation,
- hydrogenation of CO and CO_2.

They reported that nanoparticulate gold particles (5 nm) on mixed oxides have superior activity for CO oxidation at low temperatures, as shown in Table 2.1. In the $Au/MgO/MnO_x/Al_2O_3$ catalysts, MgO was thought to be the stabilizer for Au particle size, and MnO_x was the co-catalyst. The hydrogen oxidation is relatively suppressed by the multi component catalyst.

Table 2.1 Carbon monoxide and hydrogen oxidation over alumina supported gold catalysts (gold loading: 5 wt%)*

Catalyst	Average Au particle size (nm)	CO oxidation		H$_2$ oxidation	
		α(CO)	$T_{50\%}$ (°C)	α(H$_2$)	$T_{25\%}$ (°C)
Au	3.6 ± 1.4	0.22	57	0.16	63
Au/MnO$_x$	9.2 ± 2.7	0.49	35	0.19	102
Au/MgO	2.2 ± 1.0	0.59	<20	0.11	<20
Au/MgO/MnO$_x$	2.7 ± 1.0	1.00	<20	0.19	57

*Conversion α at 20°C and temperature needed for a conversion of 25% hydrogen and 50% (CO). Ratio CO/O$_2$ = 1 and H$_2$/O$_2$ = 4. Reactant flow 40 ml/min, GHSV = 2,500 h^{-1} with a mixture of H$_2$, CO and O$_2$ in helium (96 vol.%).

El et al. (2008) studied the deactivation of Au catalyst and found that it related to the build-up of stable monodentate carbonate species rather than arising from an irreversible sintering of the Au nanoparticles. These surface carbonates may either directly block active reaction sites, or the access of reaction intermediates to the active sites. Haruta and Date (2001) have observed a better performance of hemispherical Au particles as compared to more spherical shapes of around the same size. Goodman et al. (1998) have reported an inspiring result obtained by using a model Au/TiO$_2$ catalyst. As shown in Figure 2.8, turn over frequency (TOF) for CO oxidation reaches a maximum at a diameter of Au islands of 3.5 nm (3 atoms thick) where Au partially loses its metallic nature. They suggested that this transition might be correlated to the high catalytic activity. Since the sample used for catalytic activity measurements was composed of the Au islands with a certain size distribution. They summarized that the catalytic activity in CO oxidation over Au/TiO$_2$ model catalyst was dependent on the Au cluster size with a maximum occurring at about 2–3 nm.
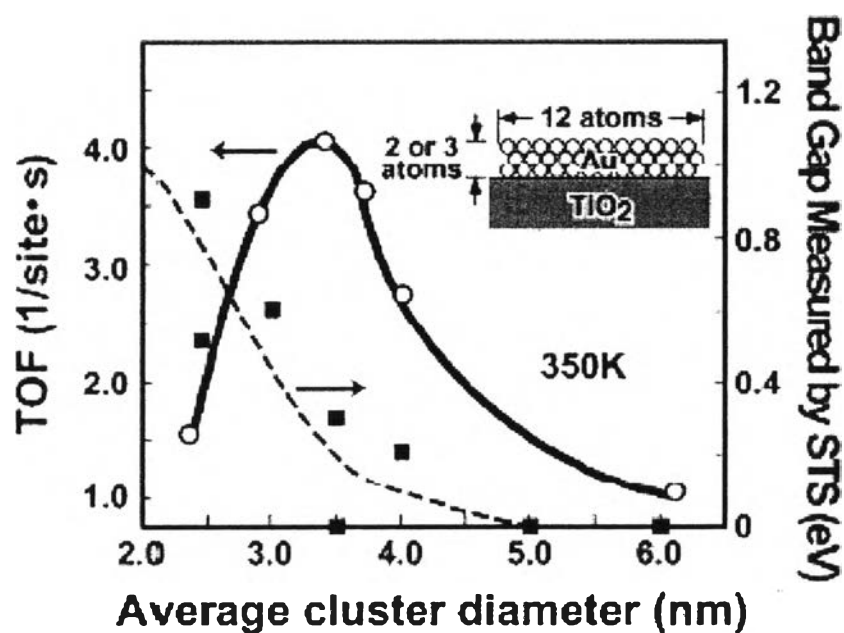
Figure 2.8 Turn over frequencies and band-gap measure by STM as a function of the diameter of Au islands deposited on TiO_2 (Goodman et al., 1998).

Another mechanism of CO oxidation on a gold particle was reported for Au/Al_2O_3, as shown in Figure 2.9 (Kung et al., 2003). However, it requires an Au^+ cation at the edge of the particle, carrying an OH^- group. An oxygen molecule adsorbs dissociatively on steps or defect sites of metallic gold atoms. A CO molecule arrives and reacts via a hydroxycarbonyl ion, liberating CO_2 and restoring the initial center. No kinetic evidence was supported of this mechanism. The existence of the $Au^I OH$ entity at the gold-alumina interface was deduced from observation on the catalyst's deactivation.
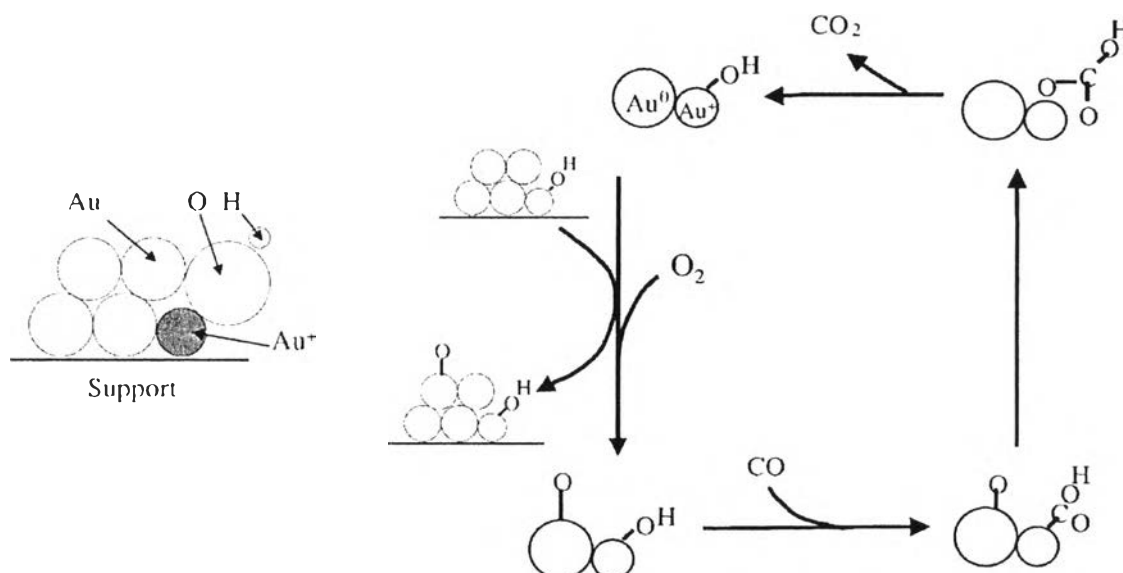
Figure 2.9 Mechanism of CO oxidation on gold particle only (Kung *et al.*, 2003).

Andreeva *et al.* (1996) reported the Au/α-Fe$_2$O$_3$ sample exhibited high catalytic activity at low temperatures in the WGS reaction and the simply mechanism of WGS reaction on Au/α-Fe$_2$O$_3$ catalysts is shown in Figure 2.10.
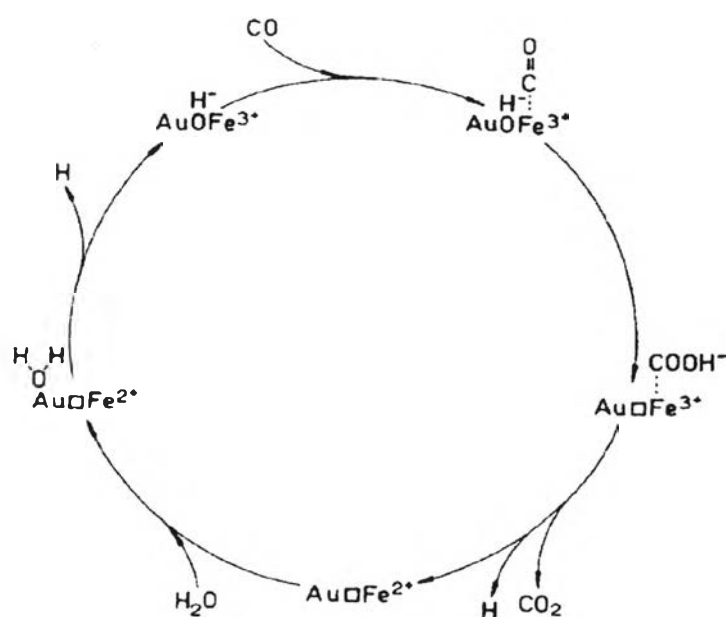

Figure 2.10 Probable scheme of the WGS reaction on the Au/α-Fe$_2$O$_3$ catalysts (Andreeva *et al.*, 1996).

2.4 Catalysts Development for Steam Reforming and Oxidative Steam Reforming of Methanol

Since SRM was introduced for hydrogen production and Cu–based catalysts were used as the efficient catalysts for SRM. However, production of hydrogen via SRM by using Cu–based catalysts still not active enough in terms of product yield and environmental concern that is the reason why many researchers are still studying the development of Cu–based catalysts.

2.4.1 Non Copper-Based Catalysts

Metals from Group 8, 9 and 10, especially Pd, are highly active in POM (Cubeiro et al., 1998). Iwasa et al. (1995) found that the catalytic performance of Pd/ZnO for SRM was shifted to higher temperature. The original catalytic functions of metallic Pd were greatly modified as a result of the formation of Pd-Zn alloys. Over the catalysts containing alloys, formaldehyde species formed in the reaction were suggested to be effectively attacked by water, being transformed into CO_2 and H_2. Chin et al. (2002) studied SRM over highly active Pd/ZnO catalyst and reported the Pd/ZnO catalysts exhibited high activity, but more importantly very low selectivity to CO for methanol steam reforming. Under the conditions examined, the decomposition activity is minimal. Easwar et al. (2005) studied the activity and selectivity pattern of ZnO and CeO_2 supported Pd catalysts in the SRM reaction. The Pd/ZnO catalysts had lower SRM rates but were more selective for the production of CO_2 than the Pd/CeO_2 catalysts. The CH_3OH conversion rates were proportional to the H_2 chemisorption uptake, suggesting that the rate determining step was catalyzed by Pd. Although Pd has higher melting point than copper and is expected to be more resistant to sintering, the stability of PdZn alloy is still an issue, and the Pd is an active catalyst for DCM, which leads to large amount of CO formation (Liu et al., 2006). Fukuhara et al. (2006) studied SRM over plate-type Pd/Zn catalyst prepared by electroless plating and found that Pd/Zn plate catalyst pretreated by reducing was more active in term of CO_2 selectivity ; however, it gave low CO selectivity, as shown in Table 2.2. Nevertheless, oxidized catalyst exhibits higher activity than reduced catalyst but it produced more CO which can poison PEM fuel cell.

Although, reduced catalyst performed low activity, its activity can increase by oxidized at various temperature after reducing as shown in Table 2.3. However, the decreasing in CO_2 selectivity of oxidizing at 500°C of plate catalyst after reducing because of formation of metallic Pd other than the PdZn alloy was also observed.

Table 2.2 Reforming performance change of the Pd-Zn catalysts by different treatment condition after plating (Fukuhara et al., 2006)

Treatment condition after plating	Reaction temperature (C)	Conversion (%)	Selectivity (%)	
			CO_2	CO
Oxidized	250	10.5	32.1	67.9
	300	43.9	41.9	58.1
	350	91.1	56.4	43.6
Reduced	250	0.2	92.7	7.3
	300	4.3	96.5	3.5
	350	35.4	97.3	2.7

The TMAB was used in the palladium plating.

Table 2.3 Reforming properties of various plate-type Pd-Zn catalysts oxidized at different temperature after reducing (Fukuhara et al., 2006)

Temperature in oxidizing (C)	Reaction temperature (C)	Conversion (%)	Selectivity (%)	
			CO_2	CO
300	300	11.4	97.3	2.7
	350	68.5	98.5	1.5
	400	91.4	96.9	3.1
400	300	27.9	93.9	6.1
	350	78.6	93.0	7.0
	400	96.8	96.1	3.9
500	300	32.0	89.4	10.6
	350	86.7	91.7	8.3
	400	96.9	89.9	10.1

The TMAB was used in the palladium plating

Yunhua *et al.* (2006) studied interaction between Pd and ZnO during reduction of Pd/ZnO catalyst for SRM and the results showed that metallic Pd is highly dispersed on ZnO. The strong interaction between Pd and ZnO during the catalyst reduction with hydrogen leads to hydrogen spillover from Pd to ZnO, which causes the reduction of ZnO closes to the metallic Pd and the formation of PdZn alloy. Accordingly, the methanol conversion and CO_2 selectivity showed a maximal value. Recently, Dagle *et al.* (2008) studied PdZnAl catalysts for the reactions of WGS, SRM, and RWGS and found that for SRM, the CO selectivities were observed to be lower than the calculated equilibrium values over a range of temperatures and steam/carbon ratios studied while the reaction rate constants were approximately of the same magnitude for both WGS and SRM. These results indicated that according to an irrelevant reaction of WGS in methanol steam reforming, $Pd/ZnO/Al_2O_3$ is not beneficial because it acts as an active WGS catalysts, WGS is not involved in methanol steam reforming. RWGS rate constants are on the order of about 20 times lower than that of SRM, suggesting that RWGS reaction could be one of the sources of small amount of CO in methanol steam reforming.

2.4.2 Copper-Based Catalysts

Although copper-based catalysts have been used in industry for the lower temperature WGS reaction, these catalysts are not suitable for automotive application of fuel cells. Since they are not active enough and they are pyrophoric, resulting in an unsuitable for start–up repeating and shut down. Therefore, many researchers started focusing on gold-based catalysts, which are very active for the low temperature WGS reaction. On the other hand, many researchers also induce Cu as a promoter to increasing catalytic activity for OSRM, this is the reason why Cu still also be using in SRM process. The catalytic activity of Cu-based catalyst almost depends on several properties of catalysts such as metal dispersion, metal surface area, and metal particle size. Although it has been proposed that there are different Cu-species with different activities. The turnover frequency based on available Cu has been shown to depend on the support such as CeO_2 giving a higher activity than Al_2O_3 (Asheim et *al.*, 2006).

Perez *et al.* (2007) studied the characterization of a commercial CuO/ZnO based catalyst for the OSRM, finding a key influence of Cu on methanol conversion, depending on the conversion rate of oxygen during the reaction. Even though, Cu-based catalysts are clearly preferred for SRM, because of their high activity and selectivity better than Pd-based catalystsat lower temperature. The traditional compositions of the commercial Cu-based SRM catalysts, the Cu/ZnO and Cu/ZnO/Al$_2$O$_3$ systems, have been previously investigated. It is generally assumed that the active sites in Cu-containing catalysts (either single atoms or particles) are in the metallic state, although the presence of Cu$_2$O species on the surface of the working catalyst has also been confirmed (Mastalir *et al.*, 2005). Liu *et al.* (2002) reported that Cu/CeO$_2$ was effective for steam reforming of methanol, as shown in Table 2.4. In addition, Zn has also exerted promoting effects for OSRM.

Moreover, Liu *et al.* (2002) also studied the effect of Cu loading versus the conversion of methanol and turnover frequency and found that Cu/CeO$_2$ have a smaller Cu particle size than other catalysts. That was the reason why the 3.9 wt% Cu/CeO$_2$ showed the highest activity for SRM. The TOF values were calculated by the surface areas of metallic Cu and the H$_2$ formation rates. The 3.9 wt% Cu/ZnO catalyst showed similar Cu particles size to the 3.9 wt% Cu/Al$_2$O$_3$ catalyst, but the TOF value of Cu/ZnO was three times higher than that of Cu/Al$_2$O$_3$ at 240 °C. This indicated that the supports influenced the catalytic activity of the catalysts. The 3.9 wt% Cu/CeO$_2$ (cop) catalyst showed the highest TOF value among the catalysts with the same Cu loading tested in this study as reported in Figure 2.11.

Table 2.4 Physical properties and TOFs for steam reforming of methanol over various catalysts

Catalyst[a]	MeOH conversion (%)[b]	BET surface area ($m^2 g^{-1}$ catalysis)	Cu surface area ($m^2 g^{-1}$ Cu)[c]	Cu particle size (nm)[c]	TOF (s^{-1})[d]
Cu/CeO$_2$ (cop)	53.9	96	101.6	6.6	0.305
Cu/ZnO	37.9	78	75.3	8.9	0.289
Cu/Zn(Al)O	32.3	114	80.8	8.3	0.230
Cu/Al$_2$O$_3$	11.2	157	73.7	9.1	0.087
Cu/CeO$_2$ (imp)	30.1	84	61.5	10.9	0.281

[a]Cu loading 3.9 wt%,

[b]Data obtained at 240 °C

[c]Measured by CO adsorption
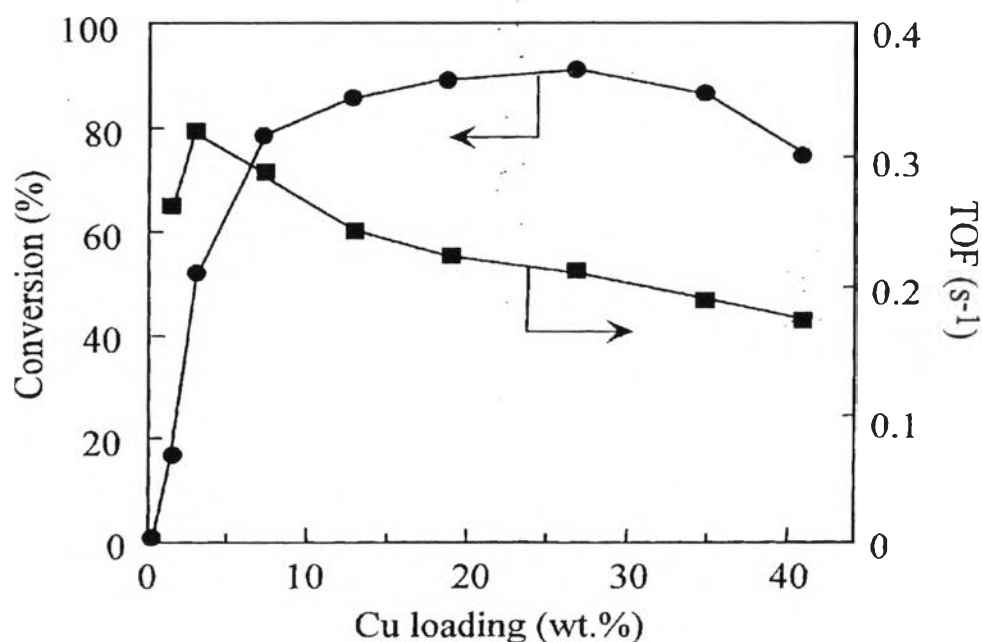
[d]Hydrogen molecules produced per surface copper atom s^{-1} at 513 K

Figure 2.11 Cu amount dependency over the Cu/CeO$_2$ (cop) catalysts for the steam reforming of methanol at 240 °C. CH$_3$OH: 0.4 atm, H$_2$O: 0.4 atm, N$_2$: 0.2 atm, and F/W: 5000 ml h^{-1} g^{-1} of catalyst.

Nevertheless, the catalytic activity of Cu–based catalysts are good enough in terms of CO and CO$_2$ selectivity ; however, rate of H$_2$ production and conversion of methanol are also considered as an main parameter. Therefore, the

maximum H_2 production and methanol conversion are firstly considered. Shishido *et al.* (2007) reported that the use of multi-component precursors may give rise to well-dispersed metal particles on the surface of oxide supports upon calcination and reduction. Methanol reacts with the surface OH groups producing methoxy species on the catalysts by elimination of water molecules already at room temperature. Moreover, the formate species are the main intermediates by increasing the temperature in the presence of pure methanol. On the contrary, undefined carbon containing species, possibly poly oxymethylene or bidentate carbonate species, are observed when the catalysts are in contact with the methanol–water–oxygen mixture at high temperatures as shown in Figure 2.12. On the other hand, the expected major activity of Cu/ZnO towards H_2 production, a lowered activity of the titania supported ones has been evidenced in the OSRM. Because titania support is related to its high selectivity towards methane formation which is a stable molecule that need high energy to remove from the catalyst surface.(Manzoli *et al.*, 2004).
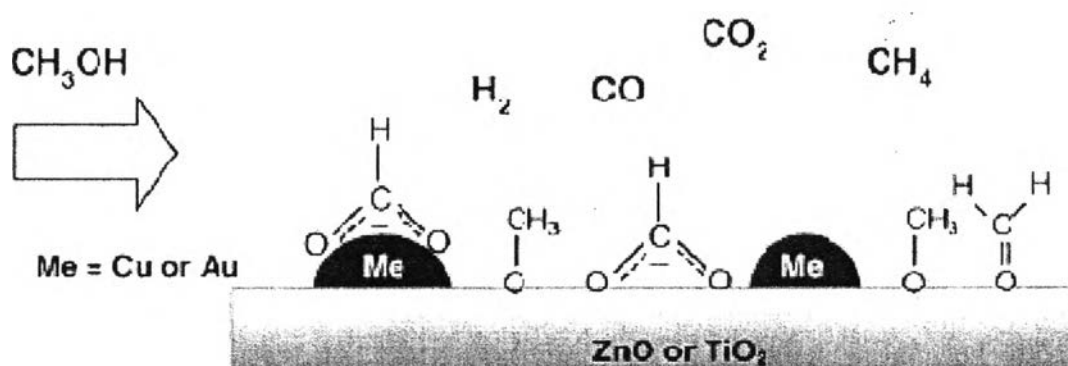

Figure 2.12 The surface species and the gaseous species produced during the DCM and CRM reaction on four catalysts (Manzoli *et al.*, 2004).
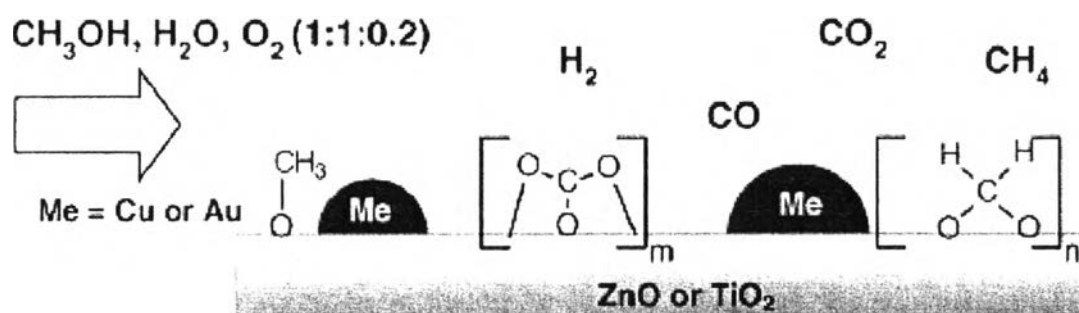
Figure 2.12 b The surface species and the gaseous species produced during the DCM and CRM reaction on four catalysts (Manzoli *et al.*, 2004).

Fierro *et al.* (1997) found that the doping of zinc into Cu/Al_2O_3 catalysts is known to limit the sintering and improving the dispersion of copper. However, Cu/ZnO based catalysts still maintain a primary interest. Patel *et al.* (2006) found that cerium promoted Cu-Zn-Ce-Al-oxide catalysts not only raised catalytic activity but also greatly increased hydrogen selectivity. Moreover, addition of cerium promoted Cu-Zn-Ce-Al-oxide catalysts also kept the CO formation very low level. Using cerium the SRM could be carried out at lower temperature with high methanol conversion, resulting in suppression of DCM and RWGS eventually end-up with the low CO and H_2-rich product stream. Cerium also stabilizes the copper–alumina catalysts effectively; which was confirmed by deactivation studies in which the Cu-Zn-Ce-Al-oxide catalysts gave the consistent performance for a long run-time compared to catalysts containing only zinc promoter. Patel *et al.* (2007) was studied OSRM over ceria promoted copper-alumina catalysts. With different loading of Ce. They found that Cu(20)CeAl obtained optimum properties of catalyst, as recorded in Table 2.5.

Table 2.5 Physiochemical properties of catalysts (Patel et al., 2007)

Cu(n)CeAl, n = wt.% of Ce →	Cu(10) CeAl	Cu(15) CeAl	Cu(20) CeAl	Cu(25) CeAl
	Cu/Ce/Al	Cu/Ce/Al	Cu/Ce/Al	Cu/Ce/Al
Composition, wt.%	30/10/60	30/15/55	30/20/50	30/25/45
Final composition, wt.%	29/9.6/ 61.4	31/14.3/ 54.7	30/19/51	29.5/26.5/ 44
BET surface area, m^2 g^{-1}	89	86	102	91
Pore volume, cm^3 g^{-1}	0.25	0.21	0.30	0.26
Cu dispersion, %	9.6	12.1	14.8	13.5
Cu surface area, m^2 g^{-1}	18.83	23.73	29.04	26.48
Cu particle size, nm	10.7	8.5	6.9	7.6
Methanol conversion[a], %	78	84	100	91
H$_2$ rate[a], mmol s^{-1} kg$^{-1}_{cat}$	139	151	179	163
CO formation[a], ppm	2068	1955	1918	1729

[a] Results at $T = 280$ °C, S/M = 1.5 M, O/M = 0.15 M and W/F = 15 kg$_{cat}$ s mol^{-1}; copper dispersion, surface area and particle size were determined using CO chemisorption.
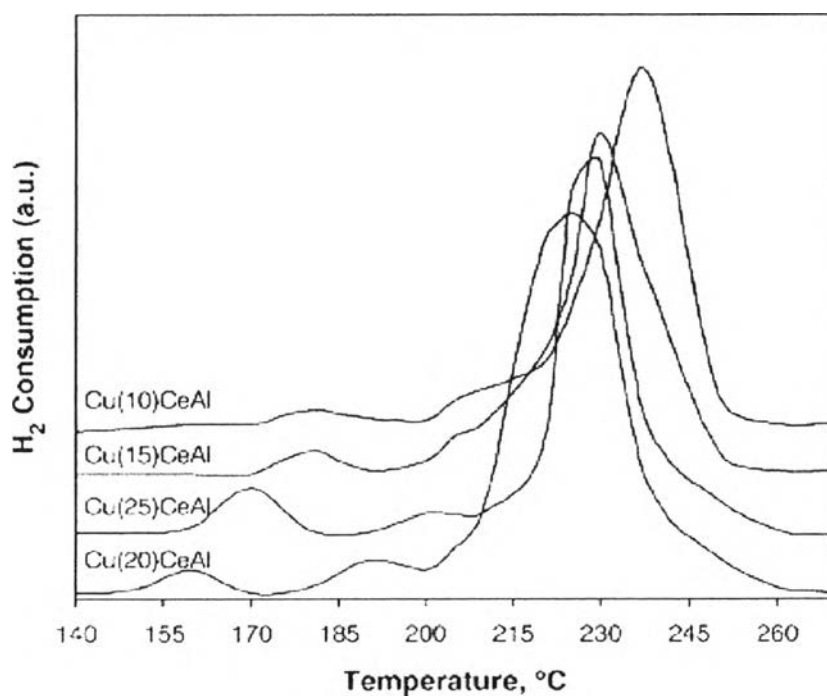

Figure 2.13 TPR spectra of calcined Cu/CeO$_2$/Al$_2$O$_3$ with various compositions (Patel et al., 2007).

From Figure 2.13 All the $Cu/CeO_2/Al_2O_3$ catalysts exhibited the three composite peaks of TPR. A first peak is attributed to the reduction of oxygen vacancies of ceria, which were generated due to the lower valent Cu species caused the structural defects of ceria lattice. The second peak was attributed to spinal $CuAl_2O_4$ and Cu_2O, and last peak was due to CuO reduction to Cu. It has been reported that at temperature lower than 170°C, peaks can be attributed to copper species strongly interacting with ceria. Catalyst Cu(20)CeAl reduced at the lowest temperature 220°C. As predicted, Cu(20)CeAl also obtained the optimum methanol conversion and H_2 production rate, as reported in Figure 2.14. It could be described that the better copper dispersion in ceria promoted copper-alumina catalyst higher than catalysts without it (Patel *et al.*, 2007).
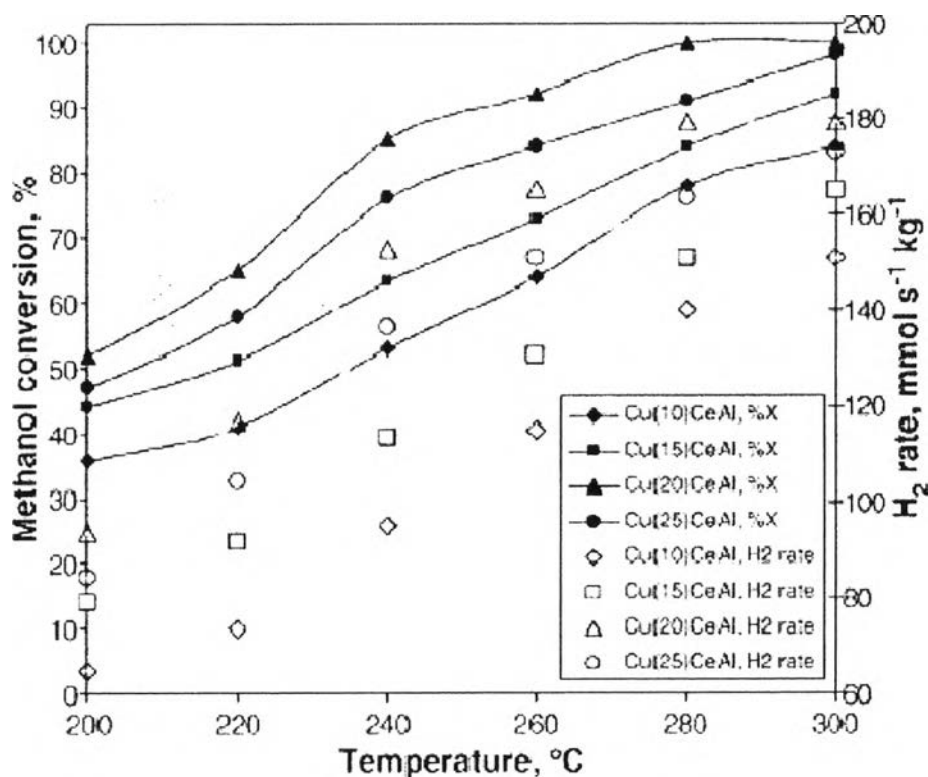

Figure 2.14 Comparison of catalytic activity for different catalysts as a function of reaction temperature (Patel *et al.*, 2007).

Optionally, Patel *et al.* (2007) also reported that contact time (F/W) also affected on methanol conversion and CO selectivity. The methanol conversion increased due to the increment of contact time, but it have to trade off with the increasing of CO formation. Recently, Pojanavaraphan. (2009) illustrated that the highest metal loading of Au/CeO_2 catalysts (5 wt%) in OSRM exhibited the highest methanol conversion of 100%, whereas the hydrogen yield was still low in the average value of 24% in the range of low-temperature (200–300°C). To continue studying the previous work, Cu metal is recommended as the promoter in Au-CuO/CeO_2 catalysts to mainly improve the catalytic activity in OSRM.